CONF-960543--2
UCRL-JC-123282
PREPRINT

Thomson Scattering in the Corona of Laser-Produced Gold Plasmas

S. H. Glenzer, C. A. Back,
K. G. Estabrook, B. J. MacGowan

This paper was prepared for submittal to the
11th Topical Conference on High Temperature Plasma Diagnostics
Monterey, California
May 12-16, 1996

May 8, 1996

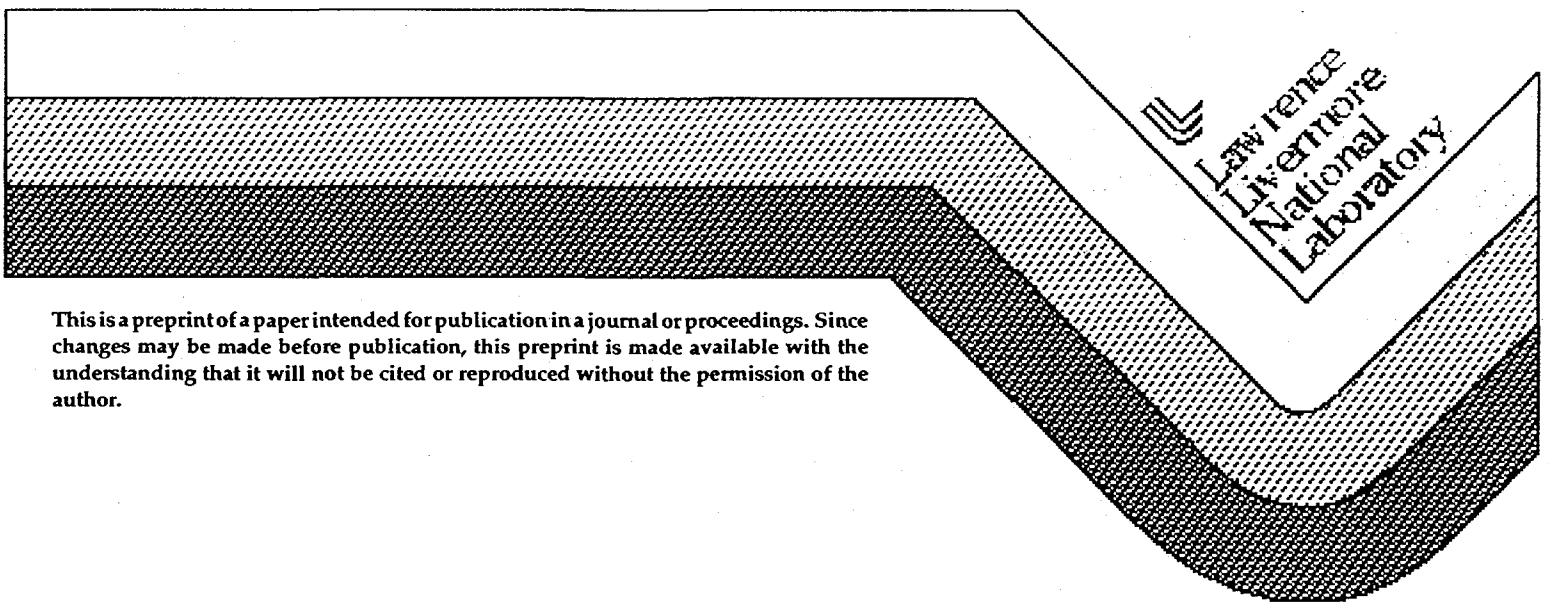

Thomson Scattering in the Corona of Laser-Produced Gold Plasmas

S. H. Glenzer, C. A. Back, K. G. Estabrook, and B. J. MacGowan
L-399, Lawrence Livermore National Laboratory, University of California P. O. Box 808, Ca 94551, U.S.A.

Thomson scattering measurements of the electron temperature in laser-produced gold plasmas are presented. We irradiated a flat gold disk target with one laser beam of the Nova laser facility. A second laser beam probed the plasma at a distance of 500 μm with temporally resolved Thomson scattering. The electron temperature measurements are compared with hydrodynamic simulations using the code LASNEX for experiments applying smoothed and unsmoothed heater beams. In case of an unsmoothed heater beam the simulations predict temperatures which are about 40% higher than our measured data. Although the agreement is improved for a smoothed heater beam, discrepancies exist in the decay phase of the plasma. We discuss possible explanations for these observations.

Random phase plates (RPPs) [1] are currently employed at large laser facilities to obtain smoothed laser beams. In particular, for future studies of indirectly driven inertial confinement fusion targets (hohlraums) at Nova, RPPs will be used for all heater beams for several reasons. For example, reducing the level of hot spots in one laser beam by a RPP yielded appreciably lower levels of stimulated Brillouin and Raman scattering in Au hohlraums and gasbags [2]. Furthermore, the characterization of methane and propane filled Au hohlraum plasmas at Nova by x-ray spectroscopy [3] showed discrepancies from hydrodynamic simulations using LASNEX [4]. We assume that these discrepancies are due to the hot spots in the laser beams whose effect on the hohlraum conditions are difficult to simulate. Significant improvements of the laser-hohlraum coupling and of the ability to predict the hohlraum plasma conditions with computer simulations are expected when RPPs are applied for all laser beams at Nova.

In this paper we describe Thomson scattering measurements of the electron temperature of Au plasmas using smoothed and unsmoothed laser beams to produce the plasma. The experimental data are compared to the two-dimensional hydrodynamic simulations, LASNEX. The results show that even in the case of a smoothed heater beam discrepancies between the simulations and experiment exist especially in the decay phase of the plasma.

The experiments were performed at the Nova laser facility. Figure 1 shows a schematic of the experimental setup. The plasma was produced by illuminating a flat disk of 2 mm diameter with a $f/4.3$ laser beam frequency converted to 3ω ($\lambda = 351.1$ nm). The angle between the heater beam and the disk normal was 64°. A 1 ns long flattop laser pulse was used with energies of 2.5 kJ. A diverging focus resulted in a spot size of 700 μm $\times$ 1,600 μm for an unsmoothed beam and 350 μm $\times$ 800 μm when using a RPP with hexagonal elements of 3 mm diameter. These spots give intensities on target of $I = 3 \times 10^{14}$ W

cm^{-2} and $I = 1 \times 10^{15}$ W cm^{-2}, respectively.

The spot size was measured with two-dimensional plasma pinhole imaging with a temporal resolution of 80 ps using gated microchannelplates. Figure 2 shows an example of the pinhole pictures of the x-ray continuum emission with $E > 2$ keV for an unsmoothed (a) and a smoothed (b) heater beam. In Fig. 2(a) significant variations of the x-ray continuum emission on a spatial scale of a few tens of microns can be seen. In addition, the central hole of the Nova laser beam can be identified. The diameter of a Nova laser beam is 65 cm before the focusing lens, and the central part with a diameter 19 cm is blocked. The laser spot shown in Fig. 2(b) obtained with a RPP has a lower level of hot spots and a rather smooth intensity distribution. Also, due to the beam smoothing the central hole disappeared.

Thomson scattering was performed with a second frequency converted 2ω ($\lambda = 526.6$ nm) laser beam at a distance of $z = 500\mu$m from the target. The probe beam was parallel to the disk and focused to a diameter of 200μm giving a scattering volume of about 200 μm $\times$ 150μm $\times$ 200μm (Fig. 1). The probe laser energies were 150 J giving probe laser intensities of 10^{14} W cm^{-2}. The Thomson scattered light was observed at a scattering angle of $\theta = 104°$ and imaged with $f/10$ optics and a 1 : 1.5 magnification onto the entrance slit of a 1m spectrometer (Spex, model 1704). Spectra were recorded with an optical streak camera (S-20) and film (Kodak, TMAX 3200) with a temporal resolution of 30 ps. A 1,200 lines/mm grating blazed at 500 nm was used in second spectral order resulting in a reciprocal linear dispersion of 0.233 nm/mm on the film. The wavelength resolution of the measurements was 0.1 nm. We performed the wavelength calibration of the detection system with Hg and Xe spectral lamps and an absolute calibration of the detector was obtained with a tungsten lamp.

Figure 3 shows the film with Thomson scattering measurements for an unsmoothed (a) and a smoothed (b) heater beam. The 3ω heater beam lasts from 0 to 1 ns and the 2ω probe beam from 0 to 4 ns. For our plasma conditions the scattering parameter is $\alpha = 1/k\lambda_D > 2$, i.e. the scattering is collective, and two ion acoustic features are easily identified on the Thomson scattering spectrum. λ_D is the Debye length and $\mathbf{k}$ is the scattering vector with $\mathbf{k} = \mathbf{k_i} - \mathbf{k_S}$ and $\mathbf{k_i} = (2\pi/\lambda_i) * \mathbf{e_i}$. λ_i is the incident probe laser wavelength and $\mathbf{e_i}$ is the unit vector in direction of the probe laser. Similarly $\mathbf{k_S}$ is in the direction of the detector. The frequency separation of the ion acoustic features is twice the ion acoustic frequency ω_{ia} of the ion acoustic waves which travel along the scattering vector $\mathbf{k}$. With the triangle relation [5] and the scattering angle of $\theta = 104°$ we obtain

$$| \mathbf{k} | = \frac{4\pi}{\lambda_i} \sin\left(\frac{\theta}{2}\right) = 1.88 \times 10^7 \quad \mathrm{m}^{-1}. \qquad (1)$$

The dispersion relation for ion acoustic waves in plasmas is given by

$$\left(\frac{\omega_{ia}}{k}\right)^2 = \frac{T_e}{M}\left(\frac{Z}{1+k^2\lambda_D^2} + \frac{3T_i}{T_e}\right), \qquad (2)$$

where T_e, T_i, Z, and M are electron and ion temperature, charge state and mass of the ions, respectively. For a highly ionized plasma or for $T_i/T_e << 1$, a condition which is often met in laser-produced plasmas, the second term in Equation (2) can be neglected. In this case the frequency separation of the ion acoustic features of the Thomson scattering spectrum gives directly the electron temperature of the plasma. Using $\Delta\lambda = 2\omega_{ia}\lambda^2/(2\pi c)$ for the wavelength separation of the ion acoustic features, we find from Eqs. (1) and (2) and with $k^2\lambda_D^2 = 0.25$

$$\Delta\lambda = 0.109\sqrt{Z\,T_e}. \qquad (3)$$

$\Delta\lambda$ is in nm and T_e in keV.

In the present study we use the charge state Z of the Au ions as calculated by LASNEX. For the laser intensities of the heater beam as applied in the present study these calculations are rather reliable. In Ref. [6] it was found that the simulations tend to overestimate Z by 10 %. This uncertainty tends to cancel out neglecting the second term in Eq. (2). We obtain electron densities with an uncertainty of about a factor of two from the simulations and the calibration of the detector. They give a scattering parameter α of 2 for our conditions. When α is approaching a value of 1 the scattering is less collective and the scattering spectrum becomes density sensitive. In this investigation, an additional error bar of 15–20% for the electron temperature is due to uncertainties in the electron density. Combining all uncertainties the electron temperature is deduced from the frequency separation of the ion acoustic features of the Thomson scattering signal with an uncertainty of 25%.

In Fig. 3(a) the Thomson scattering signal starts at $t = t_0 + 1$ ns and in Fig. 3(b) at $t = t_0 + 900$ ps, where we denote the beginning of the heating with t_0. A convenient timing and wavelength fiducial is given by the stray light signal which can be easily seen in Fig. 3(b). The timing is known to within 100 ps. The difference in the onset of the scattering signal indicates that the higher laser intensities in the case of a smoothed heater beam results in a 10% faster expansion velocity of the plasma. The plasma is moving with supersonic speed towards the observer when it reaches the scattering volume. It results in a blue shift of the Thomson scattering signal giving the opportunity to measure the instantaneous macroscopic plasma motion along the scattering vector **k**. These measurements are very accurate with an error of less than 5%. For example, in case of a smoothed heater beam we find a supersonic expansion velocity of 7×10^7 cm/s at the end of the heating at $t = t_0 + 1$ ns decreasing to 4×10^7 cm/s at $t = t_0 + 1.7$ ns. These results are in agreement with the simulations to within 10%.

Fig. 3(b) shows an increasing separation of the ion acoustic features for about 100 ps because of increasing

temperatures of the plasma for the duration of the heating. After the end of the heating at $t = t_0 + 1$ ns the separation of the ion acoustic features decreases rapidly since the plasma cools due to radiative cooling and expansion (see Fig. 3(a) and (b)). During this time the electron density in the scattering volume decreaes by only 20 % from $n_e = 1.5 \times 10^{20}\text{cm}^{-3}$ to $n_e = 1.2 \times 10^{20}\text{cm}^{-3}$, and the charge state of the Au ions is $Z = 51$ decreasing to $Z = 48$ at $t = t_0 + 2$ ns.

In Figure 4 we show the measured electron temperatures together with the results of our LASNEX simulations. We performed calculations taking into account the heater beam and the probe beam as well as only the heater beam. We discuss first the full calculations where heater and probe is included. Taking the 25% error bar of the experimental electron temperatures and the error bar of 100 ps for timing into account only a slight improvement in the agreement of experimental data and simulations is obtained when going from an unsmoothed to a smoothed heater beam. In case of the unsmoothed heater beam (Fig. 4(a)) our simulations take the hole in the center and the hot spots into account. The calculated data at $t = t_0 + 1$ ns are about 40% higher than the experimental results. In the decay phase of the plasma they are about a factor of two higher than the experiment. For a smoothed heater beam (Fig. 4(b)) the calculated peak temperature is 30% larger than obtained from the experiments. For $t_0 + 1.1$ ns $< t < t_0 + 1.4$ ns experiment and calculations agree well, and for $t > t_0 + 1.4$ ns the calculations show a factor of 2–3 larger temperatures than the experiment.

The two-dimensional LASNEX calculations for the case of an unsmoothed heater beam show significant temperature gradients close to our scattering volume, and therefore, the results are very sensitive to small errors of the location of the scattering volume which is known with an uncertainty of 30 μm. On the other hand, the calculations for the smoothed heater beam show a rather homogeneous temperature distribution. For that reason the comparison between LASNEX simulations and the experiment is less sensitive to misalignment.

Other sources of error, comparing the experiments with the modeling are: three-dimensional effects vs. two-dimensional modeling affecting the electron transport, the choice of the flux limiter affects the electron transport, and stimulated Brillouin and Raman scattering reduce the energy deposited in the plasma. The experimental spot has an aspect ratio of roughly five to one and so the temperature gradients in the short direction are roughly five times the temperature gradients in the long direction. LASNEX has two-dimensional cylindrical symmetry and assumes circular spots of the same area as the experiment. The experiment has more heat loss in the short spot direction than the LASNEX simulations. In addition, the electron transport flux limiter is semi-empirically chosen to be 0.05 and found historically to be between 0.1 and 0.03. Also, the experimental density

might be lower because of lateral expansion resulting in less inverse bremsstrahlung absorption. Further energy may be lost from stimulated Brillouin and Raman scattering. The turning point density is $n/n_c = \cos^2(\theta)$ where θ is the angle between the density gradient and the laser and n_c is the critical density. The turning point density for 64° is 0.19 which is nearly resonant for Raman scattering and the two-plasmon decay instability which can absorb laser light into hot electrons of ~50 keV. The present simulations do not account for these effects.

Our simulations show no effect of the probe laser on the plasma conditions for $t_0 < t < t_0 + 1.5$ ns (Fig. 4(b)). However, for $t > t_0 + 1.5$ ns heating of the plasma by the probe laser is predicted. Local heating of the plasma can occur when significant energy of the probe is absorbed by inverse bremsstrahlung and heat conduction is not fast enough to carry the energy away from the interaction volume. While inverse bremsstrahlung is well described by LASNEX, the classical electron transport is flux-limited by a factor of 0.05 in the present simulations. In the corona of the plasma the flux limiter might be different than in the high-density regions where it is usually measured. Too low a value for the flux limiter results in an overestimation of the effect of the probe beam on the plasma conditions. To demonstrate the effect of the probe beam on the plasma conditions as simulated by LASNEX, we also show in Fig. 4(b) a calculation neglecting the probe. In this case better agreement is obtained indicating that the probe laser heating might be overestimated in the present simulations. Further Thomson scattering experiments with a controlled variation of the probe laser energy will be necessary to study experimentally the effect of the probe on the plasma temperature for $t > t_0 + 1.5$ ns. In this way a critical experimental test of the flux limiter approximation could be performed.

In summary, Thomson scattering provides an accurate measurement of electron temperatures and plasma flow at a known position in space. We performed a comparison of electron temperatures in laser-produced Au plasmas from Thomson scattering with two-dimensional hydrodynamic simulations, LASNEX. Results of both unsmoothed and smoothed heater beams show that the temperatures are overestimated by the simulations. In case of an unsmoothed heater beam this finding could be explained by large temperature gradients. There is a slight improvement in the agreement between experiment and simulations when using a RPP to smooth the heater beam. However, discrepancies exist in the decay phase of the plasma which might be explained by an overestimation of the probe laser heating by the simulations. Further experiments testing the heat flux limiter for a corona plasma will be necessary to understand the effect of the probe laser on the plasma conditions.

The work of the Nova crew is greatly appreciated. This work was performed under the auspices of the U.S. Department of Energy by the Lawrence Livermore National Laboratory under contract No. W-7405-ENG-48.

[1] Y. Kato *et al.*, Phys. Rev. Lett. **53**, 1057 (1985). D. M. Pennington *et al.*, Proc. SPIE **1870**, 175 (1993).
[2] B. J. MacGowan, *et al.*, Phys. Plasmas **3**, 2029, (1996).
[3] C. A. Back, *et al.*, Phys. Rev. *to be published.* C. A. Back, S. H. Glenzer, O. L. Landen, and B. J. MacGowan, Rev. Sci. Instrum. (1997) *this volume.*
[4] G. Zimmerman and W. Kruer, Comments Plasma Phys. Controlled Fusion **2**, 85 (1975).
[5] H.-J. Kunze, in *Plasma Diagnostics*, edited by W. Lochte-Holtgreven (North-Holland, Amsterdam, 1968) p.550.
[6] S. H. Glenzer *et al.*, *submitted to* Phys. Rev. Lett. .

FIG. 1. Schematic of the Thomson scattering experiment. The angle between the incident heater beam and the disk normal is 64° and the scattering angle between the probe beam and the direction of observation is 104°.

FIG. 2. Example of x-ray images of the Au targets at $t = t_0 + 200$ ps. In (a) no RPP was used and in (b) the beam was smoothed with a RPP.

FIG. 3. Time-resolved Thomson scattering spectra from Au plasmas detected at a distance of 500μm from the target. In (a) no RPP was used and in (b) the beam was smoothed with a RPP.

FIG. 4. Comparison of the electron temperatures from Thomson scattering and from LASNEX simulations. In (a) no RPP was used and in (b) the beam was smoothed with a RPP. In (b) we also give a calculation without a probe laser.

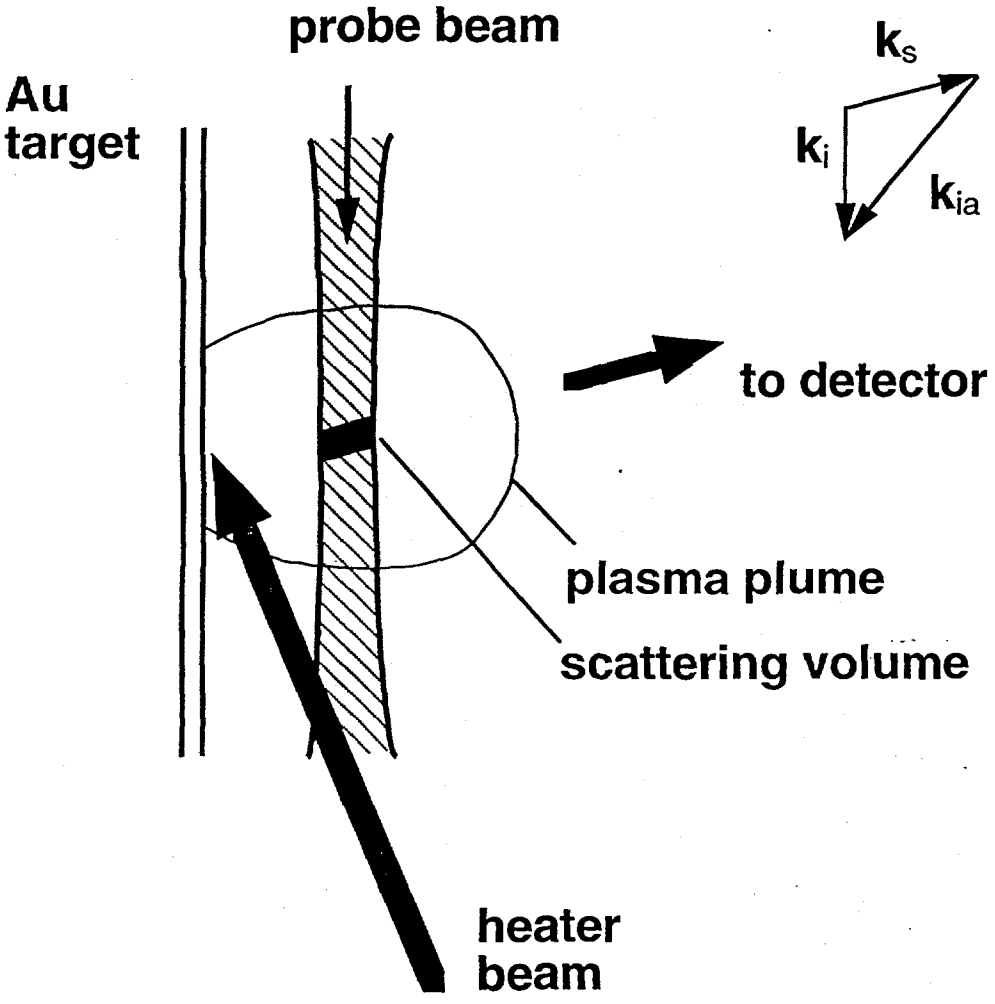
probe beam
Au
target
k_s
k_i
k_{ia}
to detector
plasma plume
scattering volume
heater
beam

Figure 1

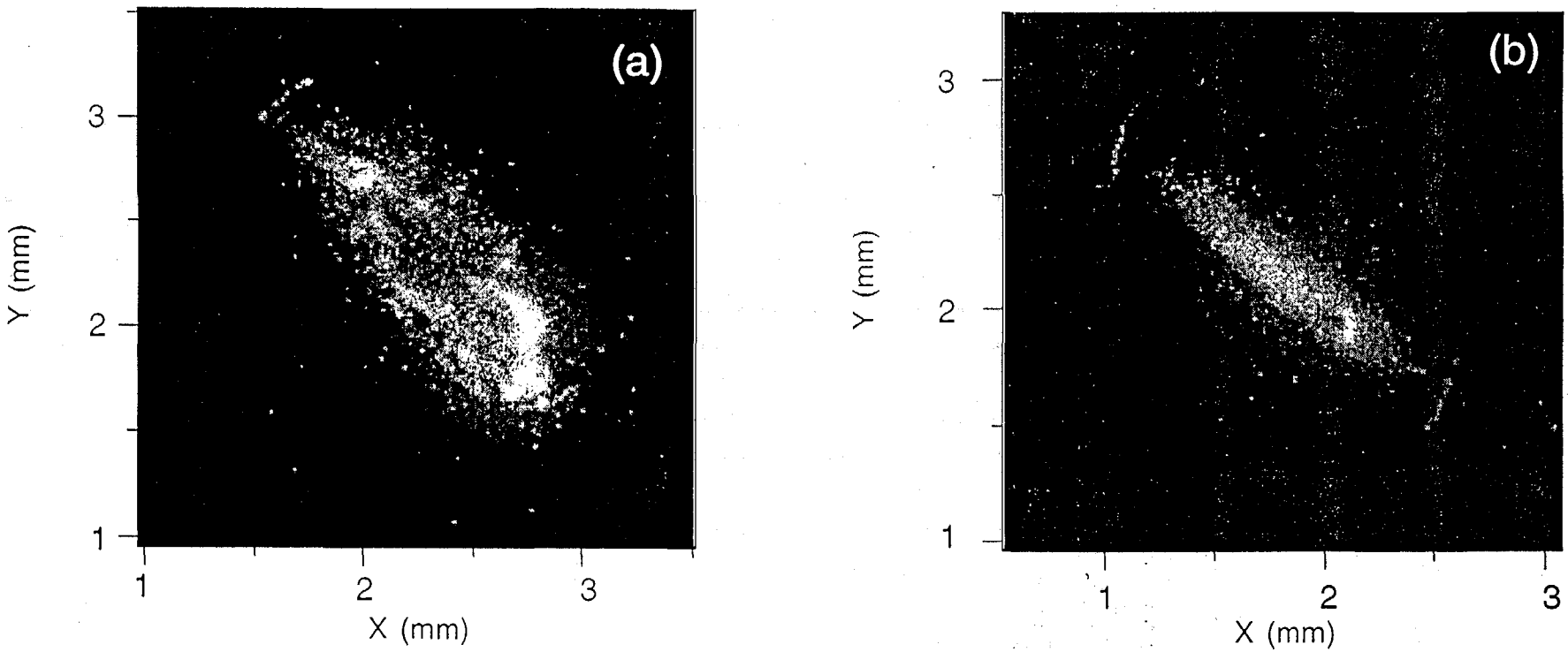

Figure 2

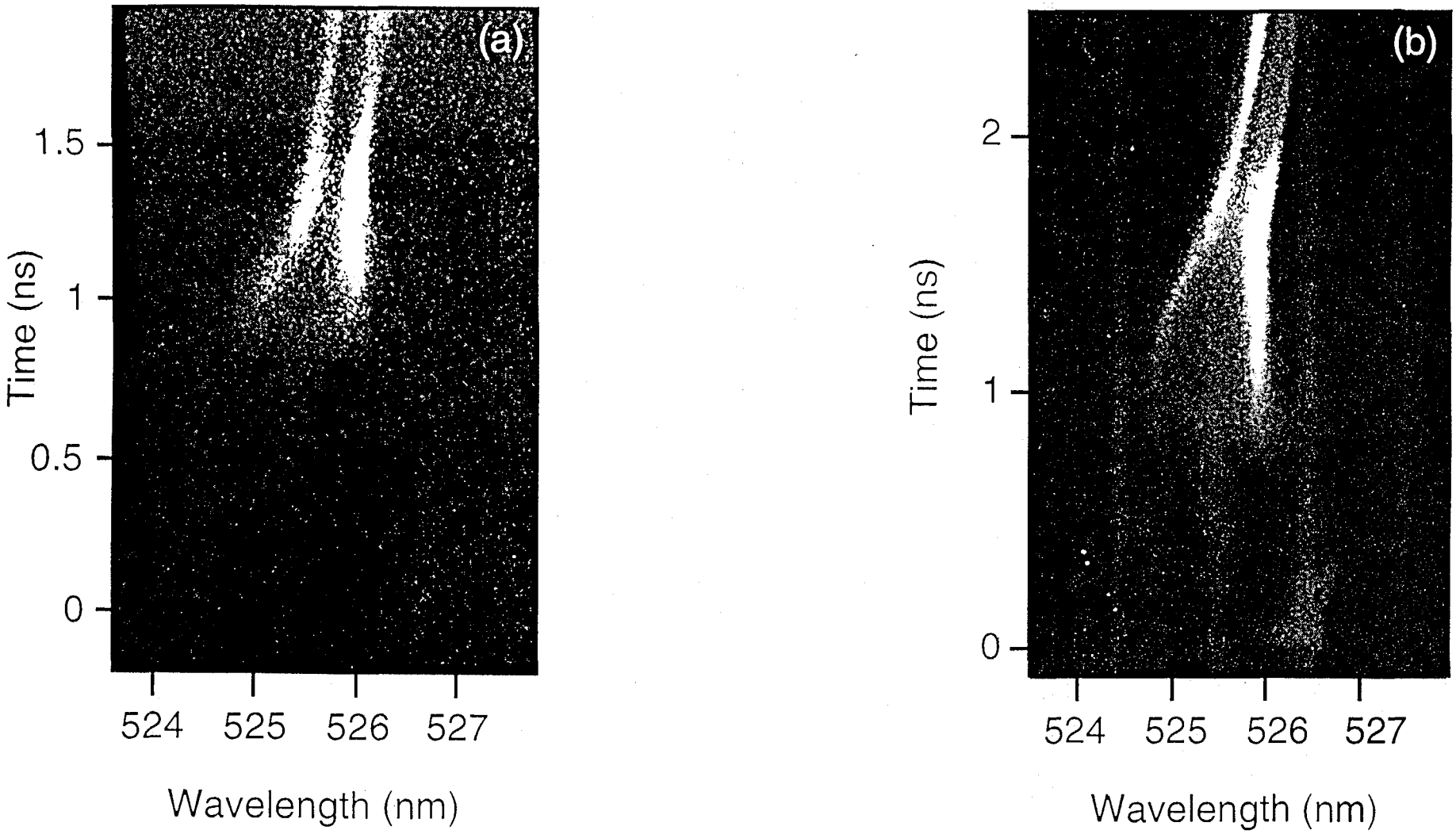

Figure 3

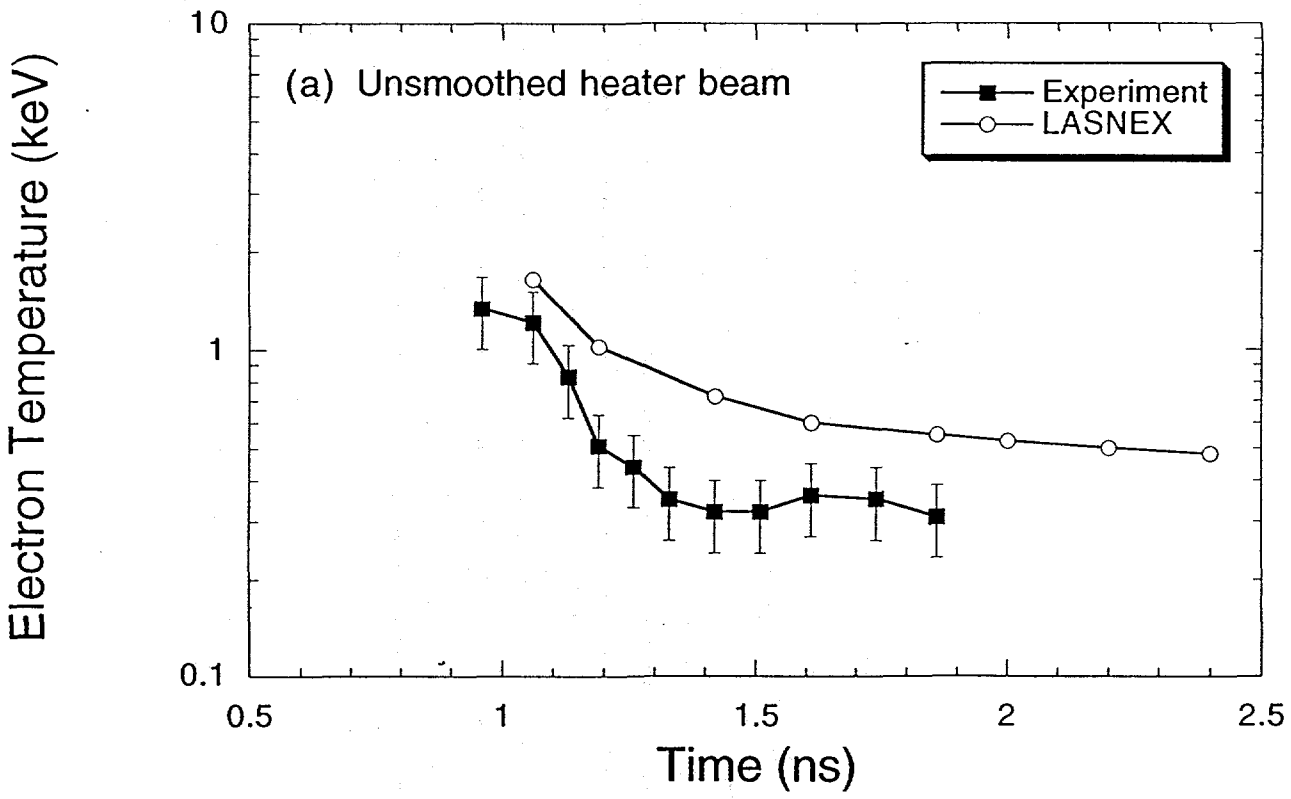
(a) Unsmoothed heater beam
Experiment
LASNEX
Electron Temperature (keV)
10
1
0.1
0.5
1
1.5
2
2.5
Time (ns)

Fig. 4a

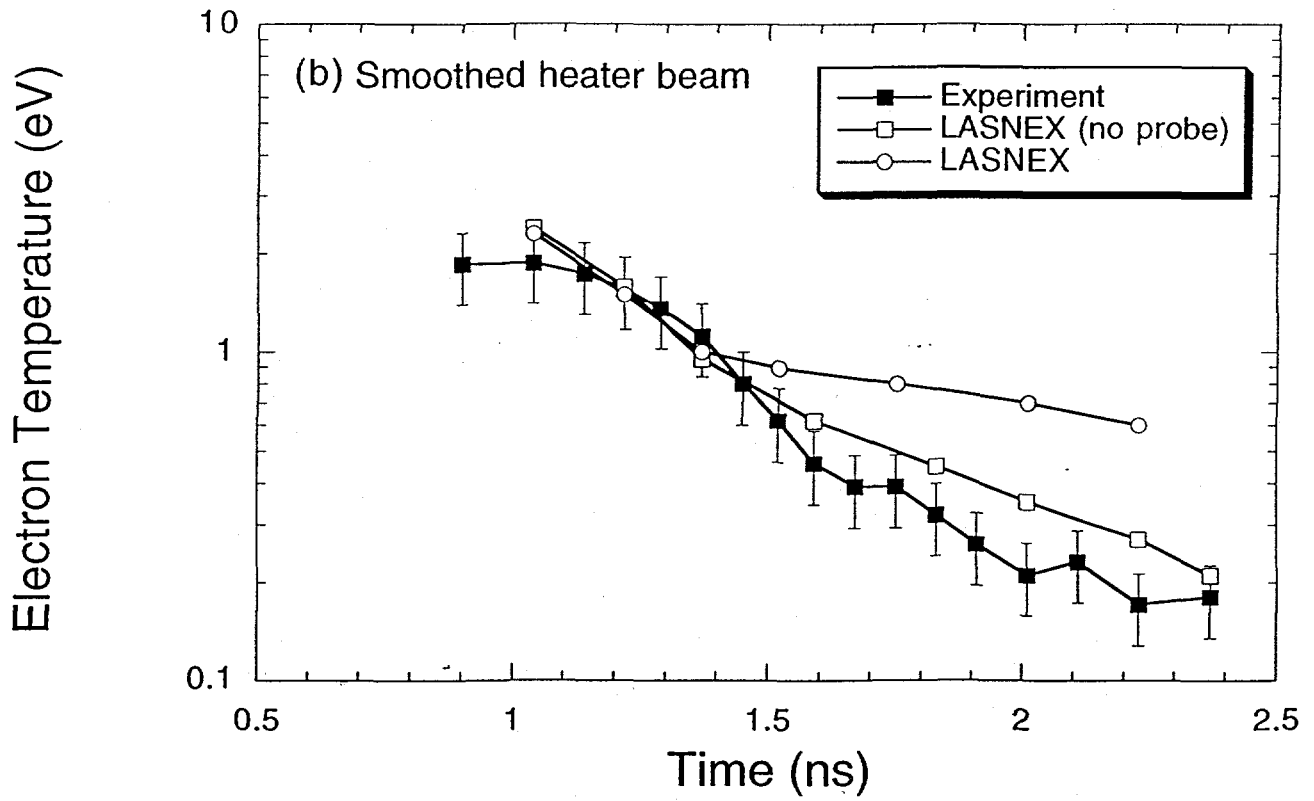
(b) Smoothed heater beam
Experiment
LASNEX (no probe)
LASNEX
Electron Temperature (eV)
10
1
0.1
0.5
1
1.5
2
2.5
Time (ns)

Fig. 46